

Multiple Bonds and Excited States from the Hartree–Fock–Heitler–London Method

Giorgina Corongiu

Dipartimento di Scienze Chimiche ed Ambientali, Università dell'Insubria, Via Lucini 3, I-22100 Como, Italy

Received: June 20, 2007; In Final Form: September 11, 2007

The recently proposed Hartree–Fock–Heitler–London, HF–HL, method (Corongiu, G. *J. Phys. Chem. A* 2006, 110, 11584) previously tested for single bond molecules is validated by potential energy computations for open and closed shells, single and multiple bonds, in ground and excited states of homopolar diatomic molecules of the first and second period. The simple HF–HL function, including the configurations for $2s/2p$ near degeneracy and avoiding state crossing, yields correct dissociation products, qualitatively correct binding, and accounts for non-dynamical correlation. Addition of ionic structures improves the ab initio HF–HL function and yields about 95% of the experimental binding energies on average. Computed excitation energies are also in agreement with laboratory values as verified for the $^3\Pi_u$ and $^3\Sigma_g^-$ excited states of the C_2 molecule. Computation of the remaining dynamical correlation using a semiempirical functional yields binding energies with an average deviation of 1.5 kcal/mol from laboratory values, and total energies with an average deviation of 0.7 kcal/mol from exact nonrelativistic dissociation energies.

1. Introduction

The variational technique provides one of the main methods used in quantum chemical computations of molecular binding. Since the beginning of theoretical chemistry, molecular orbitals (MO) and atomic orbitals (AO) one-electron functions have been recognized^{1,2} as a fundamental tool. They provide the basic starting point for the linear combination of atomic orbitals^{3–5} (LCAO) and the Heitler–London⁶ (HL) methods, and many subsequent extensions, including Hartree–Fock^{7–10} (HF); full configuration interaction^{11,12} (FCI); multi-configuration self-consistent-field^{13–19} (MC-SCF); multi-reference configuration interaction²⁰ (MRCI); natural orbitals^{21–24} (NO); alternant orbitals;²⁵ the propagator techniques;^{26,27} geminals;²⁸ and a number of valence bond^{29–36} (VB) approaches. Alternative methods do exist, such as quantum Monte Carlo,³⁷ and semiempirical approaches, which include the popular density functional techniques^{38–40} (DFT). Perturbation methods provide a parallel and efficient complement to the variational method, but they are not discussed here, as they are not directly related to variational techniques considered in this work.

The driving force for the development of many of these methods was to create quantum chemical algorithms that are computationally affordable and easy to interpret, yet provide realistic representations of bond formation and breaking. This led to the introduction of electronic correlation energy corrections,²¹ which were neglected in the two traditional models, the HF^{7–10} and HL.⁶

The Hartree–Fock–Heitler–London (HF–HL) approach is a recent quantum chemical model^{41,42} based on well-defined computational steps^{43–45} that unify and improve the HF and the HL description. The approach combines either ab initio HF and HL multi-configuration techniques,⁴³ or short ab initio HF and HL expansions with semiempirical density functional approximations.^{44,45}

In this work, I present HF–HL computations on diatomic homopolar molecules of the first and second period and, with

a simple wave function, obtain realistic binding energies from dissociation, to equilibrium separation, to the repulsive region. This demonstrates the applicability of the HF–HL method to molecules with open and closed shells, single and multiple bonds, in ground and excited states.

I start by describing the physical ideas that form the basis for the HF–HL model. Correct dissociation products are obtained by constructing the $\Psi_{\text{HF–HL}}$ wave function from a variational linear combination of HF and HL functions. If the molecule under analysis contains atoms that are nearly degenerate^{13,46–51} at dissociation and/or if the molecular state results from an avoided state crossing,⁵ then a few HF configurations and a few HL structures are added to $\Psi_{\text{HF–HL}}$ to create a wave function, called the “simple HF–HL function”, which accounts for the non-dynamical correlation energy.⁴³

The computation of the dynamical correlation energy is dealt with in post-HF–HL steps. By adding a few ionic structures to the simple $\Psi_{\text{HF–HL}}$ function, the computed molecular binding energy is improved to nearly the experimental value. This approach is based on a suggestion originally in Majorana's paper on the H_2 molecule.⁵² This work also demonstrates that ionic structures are as effective in HF–HL computations on homopolar molecules, as they are in polar molecule computations. The simple HF–HL function with the addition of ionic structures is denoted “HF–HL-ionic”, $\Psi_{\text{HF–HL–i}}$.

The remaining dynamical correlation correction can then be reduced to the sum of the correlation energies of the atoms composing the molecule. This is a nearly constant energy contribution at different internuclear separations, which can be approximated by a semiempirical density functional, the “soft Coulomb hole”.^{53–57} This functional was recently recalibrated⁵⁸ using more accurate estimates of atomic correlation energies.⁵⁹

In section 2, I provide a summary of the method, updating previous versions.^{42–45} In section 3, I list and discuss the HF configurations and HL structures used in the computations. In section 4, ab initio computations with and without ionic structures are discussed for Li_2 , Be_2 , B_2 , C_2 , N_2 , O_2 , and F_2 . In

* Corresponding author. E-mail: corongiu@uninsubria.it.

section 5, I report on the computation of the atomic component of the dynamical correlation correction.

2. The HF–HL Method

The HF–HL formal methodology^{42,43} summarized and updated below includes experience gained in this work and recent applications.^{44,45} For an n electron molecule, the HF–HL method variationally combines HF and HL wave functions, Ψ_{HF} and Ψ_{HL} :

$$\Psi_{\text{HF}} = \det(\Phi_1, \dots, \Phi_i, \dots, \Phi_n) \quad (1a)$$

$$\Psi_{\text{HL}} = \sum_k \det(\varphi_{1k}, \dots, \varphi_{jk}, \dots, \varphi_{mk}) \quad (2a)$$

Above, Φ_i defines the i th HF molecular orbital and φ_{jk} the j th atomic orbital of the k th determinant in the HL function, a VB structure; the Φ_i forms an orthogonal set, but not the φ_{jk} .

Note that the Ψ_{HL} is constructed to satisfy the correct spin coupling constraints,⁶⁰ with dissociation products into atoms in the lowest state of their ground-state configuration, subjected to satisfying Wigner–Witmer rules.⁶¹ When atoms in the molecule are in a state with near degeneracy at dissociation (e.g., 2s/2p for Be, B, and C atoms) and/or when there is an avoided state crossing,⁵ then Ψ_{HF} and Ψ_{HL} in eqs 1a and 2a can be replaced with MC–HF and/or MC–HL expansions, $\sum_s a_s \Psi_{\text{HF}}(s)$ and $\sum_t b_t \Psi_{\text{HL}}(t)$, respectively, designated Ψ_{HF} and Ψ_{HL} :

$$\Psi_{\text{HF}} = \sum_s a_s \Psi_{\text{HF}}(s) = \sum_s a_s [\det \Phi_1, \dots, \Phi_i, \dots, \Phi_n]_s \quad (1b)$$

$$\Psi_{\text{HL}} = \sum_t b_t \Psi_{\text{HL}}(t) = \sum_t b_t \sum_k [\det(\varphi_{1k}, \dots, \varphi_{jk}, \dots, \varphi_{mk})]_t \quad (2b)$$

where a_s and b_t are the coefficients of the MC expansions, and s and t characterize the length of the expansions; s and t need not be equal (see ref 43 for details).

The HF–HL wave function $\Psi_{\text{HF–HL}}$ is obtained by variational optimization of the linear expansion

$$\Psi_{\text{HF–HL}}(s,t) = c_{\text{HF}} \Psi_{\text{HF}} + c_{\text{HL}} \Psi_{\text{HL}} = \sum_s a_s \Psi_{\text{HF}}(s) + \sum_t b_t \Psi_{\text{HL}}(t) \quad (3)$$

The number of terms (s and t) of the MC–HF and MC–HL expansions differs from molecule to molecule. For the MC–HF component, in general, I use only one term, the HF ground-state configuration function. One reason for this choice is that the MC–HF configurations when added to MC–HL expansions can easily form a redundant set (the H_2 computation reported in detail in ref 43 provides a good example). Although near degenerate configurations can be selected by simple inspection of the HL terms, selection of MC–HF terms is less obvious, as the distinction between non-dynamical and dynamical correlation can be difficult; this is discussed below. State crossing configurations are an exception to this situation.

The HF function in eq 3 is either the traditional HF solution or one where the orbitals are reoptimized in the field of the MC–HL component. The number of the MC–HL terms in the HF–HL approach is discussed in section 3, where I tabulate the dissociation products generating the different MC–HL terms (structures).

In eq 3, the a_s and b_t coefficients are obtained variationally by solving the equation

$$(\mathbf{H} - \mathbf{SE})\mathbf{C} = 0$$

where \mathbf{H} and \mathbf{S} are the interaction super-matrices containing the Hamiltonian and the overlap matrix elements, respectively. The Φ_i orbitals of the Ψ_{HF} component are a linear combination of a basis set of Gaussian functions, and the same basis set is also used to expand the orbital φ_{jk} of the Ψ_{HL} component. I recall that the Φ_i orbitals form an orthogonal set, whereas the φ_{jk} orbitals can be non-orthogonal. In the latter case, following a general method proposed by Löwdin⁶² and later reinterpreted by Slater,⁶³ the interaction between two determinants, d_a and d_b , is given by:

$$\langle d_a | H | d_b \rangle = \sum_{ij} h_{ij} S^{(i,j)} + \sum_{i < k, j < l} [\langle ij | kl \rangle - \langle il | kj \rangle] S^{(i,k,j,l)}$$

where the indices i and k refer to the occupied orbitals of d_a and j and l to those of d_b ; $S^{(i,j)}$ and $S^{(i,k,j,l)}$ are the first- and second-order cofactors of the overlap matrix \mathbf{S} , constructed with the occupied orbitals of d_a and d_b . The biorthogonal transformation is an effective way to compute the cofactors,⁶⁴ but matrix element evaluation is computationally demanding. Therefore, a number of related simplifying techniques have been proposed.^{36,65} For example, Leasure et al.⁶⁶ combined determinant properties and the biorthogonal transformation, to produce an efficient evaluation of all of the matrix elements, thus reducing the complexity of the original Löwdin formulation.

In my approach, I first define the chosen HF configurations and HL structures expanded with a unique basis set of N functions. Next, I apply an integral transformation from the basis set integral list to molecular and atomic orbitals and relative cross terms between molecular and atomic functions. With algorithms used in VB literature,⁶⁵ the matrix elements $\langle d_a | H | d_b \rangle$ are then computed for the interactions of HF with HF functions, of HL with HL structures, and of HF with HL structures. I then solve by diagonalization $(\mathbf{H} - \mathbf{SE})\mathbf{C} = 0$. To optimize the orbital expansion coefficients, I currently use a numerical algorithm based on the Newton–Raphson procedure (the related computer code is still in development).⁶⁷

Equation 3 represents the first of three HF–HL successive steps, and it is referred to as the “simple HF–HL wave function”. Solutions of eq 3 produce the correct dissociation products and account for avoided curve crossing and 2s/2p near degeneracy. This means the non-dynamical component, $E_c(\text{non-dyn})$, of the correlation energy, E_c , is well represented. If I denote the dynamical component of E_c as $E_c(\text{dyn})$, then:

$$E_c = E_c(\text{non-dyn}) + E_c(\text{dyn}) \quad (4)$$

The standard definition²¹ of the correlation energy, E_c , related to HF functions, is extended⁴⁴ to include HL and HF–HL wave functions: $E_c = E(\text{n.r.}) - E_{\text{model}}$, where $E(\text{n.r.})$ is the exact nonrelativistic energy, and E_{model} refers to the energy computed via a model, like HF, HL, HF–HL, etc.

For historical reasons,^{21,68} the correlation energy correction is defined with reference to HF solutions, although the underlining expectation is to define the error implicit in any model solution relative to the exact solution of the Schrödinger equation. Again, for historical reasons, the models are de facto subdivided into those that either consider or neglect the relativistic corrections. In this work, I needed to extend the Löwdin²¹ definition, because I consider both the HF and the HL models. The relativistic correction can be considered as a small perturbation for the molecular quantities considered in this work.

Correlation correction is often partitioned by applying criteria that evaluate interaction type (short or long range) and number of electrons (two or many). Here, I apply criteria introduced in

TABLE 1: Laboratory Molecular Binding Energy (kcal/mol), E_b , Laboratory Equilibrium Distance (bohr), R_e , Total Nonrelativistic Energy (hartree) at Equilibrium, $E_T(R_e)$, and at Dissociation, $E_T(R_\infty)$, Atomic Ground-State Energies at the Hartree–Fock Limit, $E_{\text{HF}}[\text{Limit}]$, and Computed with the Basis Sets of This Work, $E_{\text{HF}}[\text{This Work}]$

molecule	E_b^a	R_e^a	$-E_T[R_e]$	$-E_T[R_\infty]^h$	$-E_{\text{HF}}[\text{limit}]$	$-E_{\text{HF}}[\text{this work}]$
H ₂ [$1^1\Sigma_g^+$]	109.48 ^b	1.40 ^b	1.1744757	1.000000	H [2^1S] 0.500000	0.499999
He ₂ [$1^1\Sigma_g^+$]	0.02 ^c	5.62 ^c	5.807483	5.807448	He [1^1S] 2.861680	2.861679
Li ₂ [$1^1\Sigma_g^+$]	24.67	5.0510	14.99543	14.95612	Li [2^1S] 7.432727	7.432721
Be ₂ [$1^1\Sigma_g^+$]	2.40 ^d	4.63 ^d	29.33860	29.33477	Be [1^1S] 14.573023	14.573016
B ₂ [$3^1\Sigma_g^-$]	68.49 ^e	3.0047	49.41695	49.30780	B [2^1P] 24.529061	24.529036
C ₂ [$1^1\Sigma_g^+$]	147.85 ^f	2.3480	75.9256	75.6900	C [3^1P] 37.688619	37.688616
N ₂ [$1^1\Sigma_g^+$]	228.4	2.0743	109.5426	109.1786	N [4^1S] 54.400934	54.400924
O ₂ [$3^1\Sigma_g^-$]	120.6	2.2819	150.3270	150.1348	O [3^1P] 74.809398	74.809384
F ₂ [$1^1\Sigma_g^+$]	39.0	2.6682	199.5305	199.4683	F [2^1P] 99.409349	99.409343
Ne ₂ [$1^1\Sigma_g^+$]	0.08 ^g	5.84 ^g	257.87673	257.8766	Ne [1^1S] 128.547098	128.547052

^a Reference 84. ^b Reference 85. ^c Reference 86. ^d Reference 87. ^e Reference 88. ^f Reference 89. ^g Reference 90. ^h Reference 59.

the early quantum chemistry literature: dynamical and non-dynamical correlation;^{46–48} Bethe–Goldstone electron pair correlation;⁶⁹ and atomic and molecular correlation components decomposition.⁷⁰ Sinanoglu’s non-dynamical correlation includes the correlation energy correction, which can be obtained from multi-configuration energy computations limited to near degenerate configurations, following Hartree et al.¹³ for Be[1^1S] and Veillard et al.⁵¹ for Be[1^1S], B[2^1P], and C[3^1P] neutral atoms and the corresponding iso-electronic series of ions.

In configuration expansions, some interactions are grouped separately. For example, on the basis of the energy difference from the reference configuration energy, I differentiate the set of nearly degenerate interactions^{13,71} from covalent or ionic higher excitations.⁷² In general, the partitioning stresses partial aspects of the correlation effects, and therefore can be incomplete and approximated, underlining that the correlation correction is a combination of different effects, often overlapping one another.

In this work, I follow a pragmatic approach, which is neither the most general nor unique, but is based on the simple application of established partitioning definitions.

It has been known since the work by Linderberg and Shull⁷¹ that the atomic near degeneracy can be related to the Z-effect and to the hydrogenic energy expression, which depends on the n , but not on the l quantum numbers ($n - l$ near degeneracy). One consequence is the atomic $2s/2p$ near degeneracy and the Z dependency of the ionic iso-electronic series for Be[1^1S], B[2^1P], C[3^1P , 1^1D , 1^1S], and N[2^1P] atoms. The $3s-3p-3d$ near degeneracy, and so on, are similar. By simply inspecting a configuration, I can decide the near degeneracy relative to a reference configuration (the ground-state configuration in this work). The atomic near degeneracy affects the molecular energy computations, because the orbital molecular correlation diagrams by Herzberg⁷³ and Mulliken⁷⁴ are built either directly with AO or with symmetry adapted linear combinations of AOs, the MO.

Alternative definitions of non-dynamical correlation have been proposed. For example, to account for the non-dynamical correlation in density functional formalisms in a Be[1^1S] study, the local scaling transformation of density functional theory was used as criterion to partition dynamical and non-dynamical correlation corrections. This led to the conclusion that the non-dynamical correlation component is 1 order of magnitude smaller than previously assumed.⁷⁵ Still another definition redefines the $2s/2p$ angular correlation as correlation of dynamical type.⁷⁶

A more general definition, unrelated to density functionals theory, has been recently advanced,⁷⁷ which provides criterion

to quantitatively establish a measure of the near degeneracy of two configurations, by comparing the computed energy of the two configurations with their interaction. This computational approach allows one to consider as near degenerate eventual configurations excluded by the simple $n - l$ near degeneracy criterion.

In this work, I consider the non-dynamical correlation for HF–HL functions, which dissociate correctly, unlike the HF function. I restrict the identification of near degenerate configurations simply to $n - l$ near degenerate configurations. Finally, I add the eventual state crossing configurations, a clear near degeneracy instance. My goal is to provide a simple but reasonable operational definition, while remaining open to the application of the above-reported “more general definition”.⁷⁷ I believe it is outside the scope of this work to compare the quality and validity of different definitions.

In the HF–HL model, the computation of dynamical correlation is dealt with in the “post-HF–HL” computations, the second and third HF–HL steps.^{42–45} In principle, I would like to correlate ab initio the valence electrons first (second HF–HL step) and then target the inner shell electrons (third HF–HL step). This can be accomplished with MC–HF^{13–19} and MC–HL expansions with large basis sets, but this approach is restricted to molecules with relatively few electrons and the computational costs are high (as shown in ref 43 for H₂ [$1^1\Sigma_g^+$], HeH [$1^1\Sigma^+$], LiH [$1^1\Sigma^+$], and BeH [$1^1\Sigma^+$]). Instead, I exploit correlation energy decompositions, like the one in eq 4 and others discussed below, to create specific components of the correlation energy to be computed either ab initio or by semiempirical density functionals.^{53–58,70,78–83}

To account for $E_c(\text{dyn})$, I make use of the decomposition into the molecular extra correlation energy,⁷⁰ η , and the sum of the correlation energy of the separated atoms $\sum_a \epsilon_a$. Recalling^{43,44} that $\eta = \eta(\text{dyn}) + \eta(\text{non-dyn})$ and $\sum_a \epsilon_a = \sum_a \epsilon_a(\text{dyn}) + \sum_a \epsilon_a(\text{non-dyn})$, I write:

$$E_c = \eta(\text{dyn}) + \sum_a \epsilon_a(\text{dyn}) + \eta(\text{non-dyn}) + \sum_a \epsilon_a(\text{non-dyn}) \quad (5a)$$

$$E_c(\text{dyn}) = \eta(\text{dyn}) + \sum_a \epsilon_a(\text{dyn}) \quad (5b)$$

Because the non-dynamical correlation is included via the simple HF–HL computation, I solve eq 5b; $\eta(\text{dyn})$ is computed ab initio and $\sum_a \epsilon_a(\text{dyn})$ and a small residual fraction of $\eta(\text{dyn})$ (discussed below in eq 6b) are approximated with density functionals.

Complementing eqs 4 and 5 I recall that, following Nesbet,⁶⁹ the correlation correction can be partitioned into the Bethe–

Goldstone decomposition, into pair correlation energies, intra-pair ω_{ii} and inter-pairs, ω_{ij} . Thus, for an n electron molecule, I write:

$$E_c = \sum_i \omega_{ii} + \sum_i \sum_j \omega_{ij} \quad (6a)$$

where in the first summation $i = 1, \dots, n/2$, and in the second, $i \neq j$. Note that, in general, $\omega_{ij} \ll \omega_{ii}$ and each pair ω can be decomposed into dynamical and non-dynamical components (see refs 43 and 44 for details). Therefore, I write:

$$E_c = \sum_i \omega_{ii}(\text{dyn}) + \sum_i \sum_j \omega_{ij}(\text{dyn}) + \sum_i \omega_{ii}(\text{non-dyn}) + \sum_i \sum_j \omega_{ij}(\text{non-dyn}) \quad (6b)$$

From eqs 4 and 6, I see that the computation of $\eta(\text{dyn})$ includes not only the intra-pair energies $\sum_i \omega_{ii}(\text{dyn})$ for binding electrons but also the elusive and small inter-pair energies $\omega_{ij}(\text{dyn})$ between binding and nonbinding electrons; the latter is the small residual fraction of $\eta(\text{dyn})$, mentioned in the discussion of eq 5b.

Finally, the molecular binding energy, E_b , can also be partitioned^{43,44} into the computed binding relative to a given quantum mechanical model, $E_b(\text{model})$, and its η_{model} :

$$E_b = E_b(\text{model}) + \eta_{\text{model}} \quad (7)$$

In HF–HL computations, η_{model} is reduced to $\eta(\text{dyn})_{\text{model}}$; below I use the shorter notation $\eta(\text{dyn})$ in place of $\eta(\text{dyn})_{\text{model}}$.

From previous computations⁴⁵ on the hydrides, I learned that a large fraction of $\eta(\text{dyn})$ can be recovered by adding to Ψ_{HL} of eq 3 a few HL ionic structures,^{34,45,52} constrained to dissociate into the lowest ionic states. In this work, I confirm the large energy gain obtained with ionic structures, but remove the constraint on the selection of the ionic structures. These are formed with products of ions in their lowest configuration, not necessarily in the lowest ionic state, and are added to the covalent HL functions of eq 3. In addition, I include, when needed, single, double, and triple ions; the ionic configurations I have selected are discussed in section 3.

The partitioning given in eqs 4–7 makes it feasible to isolate those relatively few but important HF-type functions and HL-type structures, which account for $\eta(\text{dyn})$ when added to eq 3. This strategy provides realistic binding energies, as previously reported⁴⁵ for the hydrides and for the van der Waals molecule HeH.

In the HF–HL computations, I consider the use of density functionals simply as algorithms to scale the total energy and to secure atomic correlation, nearly “an extrapolation procedure”.

From the early days of quantum chemistry,^{53–57,68,70,78–83} semiempirical functionals have been known to yield energies of different accuracy, depending partly on the functional form, but mainly on their parametrization. Today, density functional use is usually associated with DFT computations.^{1,2,38–40} Following my previous computations on hydrides, in this Article, I use the Coulomb hole, Ch, functional, specifically “the soft Coulomb hole” algorithm,^{53,54,56} recalibrated for the HF–HL energies and for near degenerate atomic energies.⁵⁸ The HF–HL wave function, $\Psi_{\text{HF–HL}}$, corrected with the soft Coulomb hole functional is designated as the HF–HL-Ch function, $\Psi_{\text{HF–HL–Ch}}$.

3. HF and HL Characterization of the HF–HL Functions

The computations performed for the homopolar molecules are obtained with basis sets⁴³ large enough to reach the Hartree–

TABLE 2: Atomic and Ionic States for the HF–HL Functions at Dissociation

H ₂ [¹ Σ _g ⁺] atomic	cationic	anionic
[1] H [² S](1s ¹)	[1] H ⁺ (1s ⁰)	[1] H ⁻ [¹ S](1s ²)
		[2] H ⁻ [¹ S](2p ²)
		anionic
He ₂ [¹ Σ _g ⁺] atomic	cationic	
[1] He [¹ S](1s ²)		
Li ₂ [¹ Σ _g ⁺] atomic	cationic	anionic
[1] Li [² S](1s ² 2s ¹)	[1] Li ⁺ [¹ S](1s ²)	[1] Li ⁻ [¹ S](1s ² 2s ²)
Be ₂ [¹ Σ _g ⁺] atomic	cationic	anionic
[1] Be [¹ S](2s ²)	[1] Be ⁺ [² S](2s ¹)	[1] Be ⁻ [² S](2s ² 3s ¹)
[2] Be [³ P](2s ¹ 2p ¹)	[2] Be ⁺ [² P](2s ⁰ 2p ¹)	[2] Be ⁻ [² S](2s ¹ 3s ²)
[3] Be [¹ S](2s ⁰ 2p ²)		[3] Be ⁻ [² P](2s ² 2p ¹)
[4] Be [¹ D](2s ⁰ 2p ²)		[4] Be ⁻ [² S](2s ¹ 2p ²)
[5] Be [³ P](2s ⁰ 2p ²)		[5] Be ⁻ [² P](2s ⁰ 2p ³)
B ₂ [³ Σ _g ⁻] atomic	cationic	anionic
[1] B [² P](2s ² 2p ¹)	[1] B ⁺ [¹ S](2s ²)	[1] B ⁻ [³ P](2s ² 2p ²)
[2] B [² P](2s ⁰ 2p ³)	[2] B ⁺ [³ P](2s ⁰ 2p ²)	[2] B ⁻ [³ P](2s ¹ 2p ³)
[3] B [² D](2s ⁰ 2p ³)	[3] B ⁺ [³ P](2s ¹ 2p ¹)	[3] B ⁻ [¹ S](2s ¹ 2p ³)
[4] B [² P](2s ¹ 2p ²)	[4] B ⁺ [¹ S](2s ⁰ 2p ²)	[4] B ⁻ [¹ D](2s ¹ 2p ³)
[5] B [² D](2s ¹ 2p ²)		
C ₂ [¹ Σ _g ⁺] atomic	cationic	anionic
[1] C [³ P](2s ² 2p ²)	[1] C ⁺ [¹ S](2s ² 2p ⁰)	[1] C ⁻ [¹ S](2s ² 2p ⁴)
[2] C [¹ S](2s ² 2p ²)	[2] C ⁺ [¹ S](2s ⁰ 2p ²)	[2] C ⁻ [¹ D](2s ² 2p ⁴)
[3] C [¹ D](2s ² 2p ²)	[3] C ⁺ [¹ D](2s ⁰ 2p ²)	[3] C ⁻ [³ P](2s ² 2p ⁴)
[4] C [³ P](2s ¹ 2p ³)	[4] C ⁺ [³ P](2s ⁰ 2p ²)	[4] C ⁻ [³ P](2s ¹ 2p ⁵)
[5] C [³ P](2s ⁰ 2p ⁴)	[5] C ⁺ [³ P](2s ¹ 2p ¹)	[5] C ⁻ [² P](2s ² 2p ³)
[6] C [¹ S](2s ⁰ 2p ⁴)	[6] C ⁺ [² P](2s ¹ 2p ²)	[6] C ⁻ [² D](2s ² 2p ³)
[7] C [¹ D](2s ⁰ 2p ⁴)	[7] C ⁺ [² S](2s ¹ 2p ²)	[7] C ⁻ [² S](2s ¹ 2p ⁴)
	[8] C ⁺ [² D](2s ¹ 2p ²)	[8] C ⁻ [² D](2s ¹ 2p ⁴)
		[9] C ⁻ [² P](2s ¹ 2p ⁴)
		[10] C ⁻ [² P](2s ⁰ 2p ⁵)
		anionic
N ₂ [¹ Σ _g ⁺] atomic	cationic	
[1] N [³ S](2s ² 2p ³)	[1] N ⁺ [³ P](2s ² 2p ²)	[1] N ⁻ [³ P](2s ² 2p ⁴)
[2] N [² D](2s ² 2p ³)	[2] N ⁺ [¹ D](2s ² 2p ²)	[2] N ⁻ [¹ D](2s ² 2p ⁴)
	[3] N ⁺ [¹ S](2s ² 2p ²)	[3] N ⁻ [¹ S](2s ² 2p ⁴)
	[4] N ⁺ [² P](2s ² 2p ¹)	[4] N ⁻ [² P](2s ² 2p ⁵)
	[5] N ⁺ [³ S](2s ² 2p ⁰)	[5] N ⁻ [³ S](2s ² 2p ⁶)
		anionic
O ₂ [³ Σ _g ⁻] atomic	cationic	
[1] O [² P](2s ² 2p ⁴)	[1] O ⁺ [² P](2s ² 2p ³)	[1] O ⁻ [² P](2s ² 2p ⁵)
[2] O [¹ D](2s ² 2p ⁴)	[2] O ⁺ [³ P](2s ² 2p ²)	[2] O ⁻ [¹ S](2s ² 2p ⁶)
[3] O [¹ S](2s ² 2p ⁴)		
F ₂ [¹ Σ _g ⁺] atomic	cationic	anionic
[1] F [² P](1s ² 2s ² 2p ⁵)	[1] F ⁺ [¹ D](1s ² 2s ² 2p ⁴)	[1] F ⁻ [¹ S](1s ² 2s ² 2p ⁶)
Ne ₂ [¹ Σ _g ⁺] atomic	cationic	anionic
[1] Ne [¹ S](1s ² 2s ² 2p ⁶)		

Fock limit energy for the atoms. These basis sets are augmented with polarization functions to ensure molecular energies close to the Hartree–Fock limit and accurate CASSCF expansions.⁴³

In Table 1, for the homopolar diatomic molecules, I report laboratory binding energy (kcal/mol), E_b , laboratory equilibrium distance (bohr), R_e , total nonrelativistic energy (hartree) at equilibrium, $E_T(R_e)$, at dissociation, $E_T(R_\infty)$, Hartree–Fock limit for the separated atoms, $E_{\text{HF}}[\text{limit}]$, and the HF energy computed with the basis set of this work, $E_{\text{HF}}[\text{this work}]$. The nonrelativistic energies $E_T(R_\infty)$ are obtained from the carefully estimated atomic energies by Chakravorty et al.;⁵⁹ the total nonrelativistic energies $E_T(R_e)$ are obtained by adding E_b to $E_T(R_\infty)$.

In Table 2, I report the atomic state functions (neutral and ionic) used to build the dissociation products of the HF–HL functions (constrained by the Wigner–Witmer rules). For Be₂,

TABLE 3: Computed (at the Experimental Geometries) Ab Initio Binding Energy (kcal/mol), E_b , Total Energy (hartree), E_t , and Correlation Energy (hartree), E_c , for HF, HL, HF–HL(S,T), and HF–HL- i Models (Experimental Binding Energies (kcal/mol), $E_b(\text{exp})$, Are Also Reported)

binding	Li ₂	Be ₂	B ₂	C ₂	N ₂	O ₂	F ₂
$E_b(\text{HF})$	3.83	-7.54	20.53	18.27	120.15	30.18	-29.24
$E_b(\text{HL})$	8.68	-19.23	-15.59	-0.92	121.96	1.51	-17.59
$E_b(\text{HF–HL})(1,1)$	8.69	-7.53	23.05	41.90	159.96	62.26	11.46
$E_b(\text{HF*–HL})(1,1)$ (S,T)	8.80 (1,1)	-7.48 (1,5)	25.58 (1,5)	53.68 (1,7)	164.19 (1,2)	65.58 (1,3)	15.43 (1,1)
$E_b(\text{HF–HL})(S,T)$	21.84 ^a	-9.49	55.01	127.10	175.04	76.56	11.46
$E_b(\text{HF*–HL})(S,T)$	21.87	-8.56	56.07	134.38	178.96	82.11	15.43
$E_b(\text{HF–HL-}i)$	25.48 ^b	0.50	62.95	138.40	213.16	110.12	35.70
$E_b(\text{HF*–HL-}i)$	25.70	0.52	63.77	143.86	220.03	115.02	38.71
$E_b(\text{exp})$	24.67	2.40	68.49	147.85	228.4	120.6	39.0
total							
$E_t(\text{HF–HL})R_\infty$	14.86544	29.23347	49.12360	75.41206	108.80184	149.61924	198.81916
$E_t(\text{HF–HL})R_c$	14.87929	29.21834	49.21126	75.61460	109.05677 ^b	149.71845 ^c	198.83742
$E_t(\text{HF–HL-}i)R_c$	14.90604	29.23427	49.22392	75.63262	109.14154	149.79473	198.87700
correlation							
$E_c(\text{HF})$	0.12389	0.20458	0.32615	0.51925	0.54927	0.66014	0.75841
$E_c(\text{HL})(T)$	0.11616	0.12101	0.20569	0.31120	0.54640	0.70536	0.73942
$E_c(\text{HF–HL})(S,T)$	0.11614	0.12026	0.20169	0.31100	0.48584	0.60855	0.69308
$E_c(\text{HF–HL-}i)$	0.08939	0.10433	0.19303	0.29298	0.40106	0.53227	0.65350

^a This value is obtained with a MC–HL containing four structures. ^b The value reported corresponds to the (1,1) computation. The values for the (1,2) case are: $E_t(\text{HF–HL})(R_c) = -109.08077$ hartree, and $E_b(\text{HL})(2) = 163.58$ kcal/mol. ^c The value reported corresponds to the (1,1) computation. The values for the (1,3) case are: $E_t(\text{HF–HL})(R_c) = -149.74078$ hartree, and $E_b(\text{HL})(3) = 54.53$ kcal/mol.

B₂, and C₂ to the neutral atomic states of the $1s^2 2s^2 2p^n$ configurations, I add states of the near degenerate configurations $1s^2 2s^0 2p^{n+2}$ and $1s^2 2s^1 2p^{n+1}$ (and equivalently for the ionic configurations). Note the limited number of states used to create the HL structures. From the table, it is easy to see how the number of states might be increased, but I purposely kept it small to show the impact of a few well-chosen states mainly belonging to the lowest configuration. For the HF component of the HF–HL function, I have restricted my choice to the ground-state function of the ground-state configuration, tabulated for example in Herzberg’s classical volume.⁵

To demonstrate the use of Table 2, I consider the O₂ molecule. The HF–HL(1,1) function is simply the combination of the HF ground-state function and of the HL function generated by “atomic” state labeled [1] in the first column of the table, 3P – 3P . The notation HF–HL(S,T), which relates to HF configurations and HL structures, should not be confused with the one of eq 3, where the indices s and t refer to the number of component functions in the HF–HL wave function. The (HF–HL)(1,3) function is obtained by adding to (HF–HL)(1,1) the HL covalent structures generated from the combination of “atomic” states labeled [1] and [2] in the table and from the combination of “atomic” states labeled [1] and [3], thus 3P – 3P , 3P – 1D , and 3P – 1S . The (HF–HL- i) function is obtained by adding ionic structures to (HF–HL)(1,3): these are a combination of the “cationic” state labeled [1] with the “anionic” state labeled [1] and also of the “cationic” state labeled [2] with the “anionic” state labeled [2], $O^+[^2P]$ – $O^-[^2P]$, $O^{+2}[^3P]$ – $O^{-2}[^3P]$; thus, the (HF–HL)(1,3) function is composed by a total of 4 HL structures and the (HF–HL- i) by a total of 8 structures. It is evident that the number of covalent and/or ionic structures can be easily increased to yield computed binding energies even closer to the experimental value than those reported in this work.

However, the so-called “ionic structures” raise the physical interpretation problem pointed out in 1931 by Majorana:⁵² charge transfer via ionic structures has no physical interpretation in homopolar molecules. The ionic structures are simply an efficient way to introduce “in–out” correlation. Majorana used the designation “pseudo-polar”; I shall continue with the use of the term “ionic structure”, following the VB tradition.

4. Ab Initio Computation of Binding Energy for Ground and Excited States

In this section, I report on the ab initio HF–HL computations, with and without ionic structures (limited to those constructed with the data in Table 2). If in HF–HL computations the orbitals of the HF component are frozen to the HF solution, I use the notation HF–HL, if reoptimized in the field of the HL structures I use the notation HF*–HL. Therefore, I shall discuss HF–HL(1,1), HF*–HL(1,1), HF–HL(S,T), HF*–HL(S,T), HF–HL- i , and HF*–HL- i computations, summarized in Table 3, where the experimental binding energies have been added. In Figure 1, I report the potential binding energy curves computed with the HF, HL, and simple HF–HL wave functions (eq 3), without inclusion of $2s/2p$ near degeneracy effects. For computations with interactions between structures generated from atomic ground states and from atomic excited states (of the same atomic ground-state configuration) like in N₂ and O₂, see Table 2 first column case [1] and [2] for N₂ and [1], [2], and [3] for O₂, the two lowest solutions are indicated with the letters a (lower state) and b (higher state). In the figure, I use the notation HF–HL(S,T), except for the case where $S = T = 1$, to avoid a redundant notation. Each potential energy curve is computed at 30–40 internuclear separations, and the reported dissociation energy values are computed at internuclear separation of 40 bohr.

The binding energies for H₂ are those reported in ref 45, with $E_b(\text{HF–HL})(1,1) = 83.83$ kcal/mol and $E_b(\text{HF–HL-}i)(1,2) = 100.24$ kcal/mol. For H₂ and Li₂, the binding energy from the Ψ_{HL} function is essentially equal to that from $\Psi_{\text{HF–HL}}$, and both are superior to the Ψ_{HF} binding energy. For Be₂ and B₂, the binding energy improves from Ψ_{HL} (which yields repulsive potential energy curves) to Ψ_{HF} to $\Psi_{\text{HF–HL}}$ to $\Psi_{\text{HF*–HL}}$. From Figure 1, I see that the HF–HL approximation (even without inclusion of $2s/2p$ near degeneracy) is definitely superior to the HF and HL approximations.

For C₂, the HL approximation is rather poor at equilibrium; it improves in the HF model and notably so in HF–HL and HF*–HL computations.

For N₂, the HF and HL approximations yield essentially the same binding energy value, which improves significantly with the use of the HF–HL and HF*–HL approximations, and even

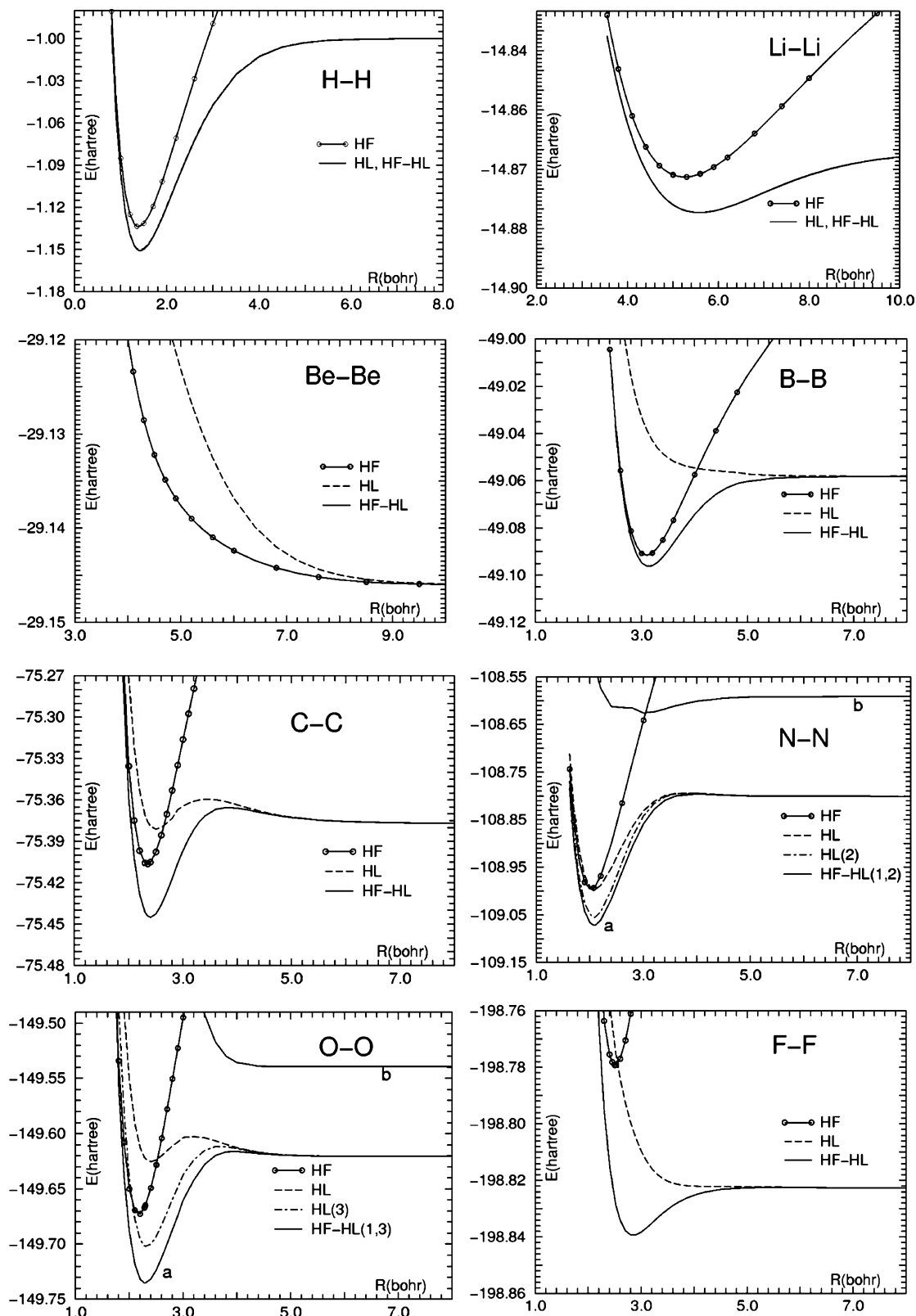


Figure 1. HF, HL, and HF-HL first step potential energy curves, without near degeneracy, for the ground state of H_2 , Li_2 , Be_2 , B_2 , C_2 , N_2 , O_2 , F_2 , and state interactions for N_2 and O_2 .

more when the interaction with a second HL structure is included (see Table 2) leading to the curve HF-HL(1,2)a. The binding computed with HF*-HL-i reaches the value of 220.03 kcal/mol.

The same situation holds for O_2 (see Figure 1), where the HF-HL(1,3) function results from the linear combination of $O(^3P)-O(^3P)$, $O(^3P)-O(^1D)$, and $O(^3P)-O(^1S)$, leading to three

solutions, designed a, b, and c (the latter is not reported in the figure because it is too high in energy). The HL(1) potential energy presents a small energy bump before dissociation, which is notably reduced in the lower solution, curve labeled a. The HF*-HL-i binding energy is 115.02 kcal/mol.

For the F_2 molecule, the HF binding energy, the well-publicized Achilles' heel of the HF method, is strongly repulsive

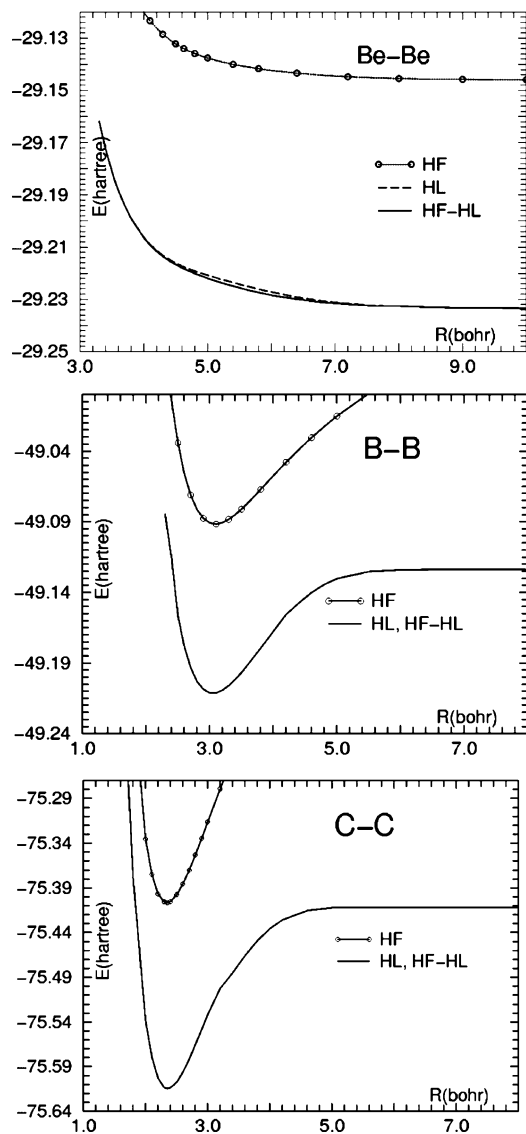


Figure 2. HF(1), HL, and HF–HL with near degeneracy: potential energy curves for the ground state of Be_2 , B_2 , and C_2 .

both in the HF and in the HL models. On the contrary, the HF–HL method yields an attraction, 11.46 kcal/mol, without reoptimization of the HF orbitals in the field of the HL structure, and 15.43 kcal/mol after reoptimization. I recall that two determinant MC–HF computations yield binding, 12.45 kcal/mol by Das and Wahl⁹¹ and 14.99 kcal/mol by Lie and Clementi.⁹²

The HF–HL method is clearly an improvement over the HF and HL methods, and it provides qualitative agreement with experimental binding. The assumption that the HF component always prevails at relatively short distances, whereas the HL always at large distances, is brought into question by the data in ref 42, which shows the computed coefficients a and b of eq 3. The implication is that two methods co-exist for much of the binding region and complement each other.

The effect of near degeneracy for Be_2 , B_2 , and C_2 is substantial, shown by the potential energy curves of Figure 2. For C_2 , I have in addition considered the $^3\Pi_u$ and $^3\Sigma_g^-$ excited states; experimentally,^{84,89} the lowest state is the $^1\Sigma_g^+$, followed by the $^3\Pi_u$ with an excitation energy of 0.1 eV and by the $^3\Sigma_g^-$ with an excitation energy of 0.96 eV. The HF–HL binding of the $^1\Sigma_g^+$, $^3\Pi_u$, and $^3\Sigma_g^-$ states, without inclusion of near degeneracy,

is 41.90, 83.72, and 100.61 kcal/mol, respectively. This can be compared to the HF values of 18.27, 72.94, and 87.34 kcal/mol and to the experimental values^{84,89} of 147.85, 143.51, and 126.91 kcal/mol. The HF–HL total energies are -75.44406 , -75.51065 , and -75.53767 hartree for the three states $^3\Sigma_g^+$, $^3\Pi_u$, and $^3\Sigma_g^-$, respectively. Note the incorrect trend in the excitation energies. Inclusion of near degeneracy improves the binding energies to 127.10, 124.06, and 107.30 kcal/mol with total energies of -75.61460 , -75.60967 , and -75.58305 hartree for the three states $^1\Sigma_g^+$, $^3\Pi_u$, and $^3\Sigma_g^-$, respectively. Note that inclusion of near degeneracy leads to a correct order of the excitation energies, 0.13 and 0.86 eV for the $^3\Pi_u$ and $^3\Sigma_g^-$, respectively; the 0.13 eV value improves previous⁹³ MC–HF results. In Figure 3, left inset, I display the three states without and with inclusion of near degeneracy. Recalling the importance of near degeneracy in the CH study,⁴³ and considering the data from Figure 3, I conclude that carbon chemistry is notably influenced by near degeneracy.

Table 3 reports the binding energy (in kcal/mol) obtained from the HF, HL, HF–HL(1,1), HF–HL(S,T), and HF–HL- i computations, indicated as $E_b(\text{HF})$, $E_b(\text{HL})$, $E_b(\text{HF–HL})(1,1)$, $E_b(\text{HF–HL})(S,T)$, and $E_b(\text{HF–HL-}i)$, respectively, and $E_b(\text{HF*–HL})(1,1)$, $E_b(\text{HF*–HL})(S,T)$, and $E_b(\text{HF*–HL-}i)$. In Table 3, I also report the total energy from HF–HL at equilibrium, $E_t(\text{HF–HL})(R_e)$, and at dissociation, $E_t(\text{HF–HL})(R_\infty)$, and the total energy at equilibrium for HF–HL- i , designated $E_t(\text{HF–HL-}i)(R_e)$. The improvement due to the inclusion of the ionic structures is large as shown from the values of $E_b(\text{HF–HL-}i)$ and $E_b(\text{HF*–HL-}i)$ reported in the table. The computed binding energy results confirm the conclusion from my hydride study:⁴⁵ ab initio HF–HL computations with the addition of ionic structures yield realistic binding values from wave functions with short expansions. Now I can extend that conclusion from single to multiple bond molecules, from ground to excited states. In the HF–HL- i computations for Li_2 , the ionic structure includes the negative ion Li^- ($1s^2 2s^2$), near degenerate with Li^- ($1s^2 2p^2$); thus, because the basis set includes 2p functions, in $E_b(\text{HF–HL-}i)$ there is some near degeneracy gain, which accounts for the 0.82 kcal/mol, seemingly overestimating the experimental value near equilibrium, but not at dissociation, where the ionic structure does not contribute.

In a recent computation,⁹⁴ the ground state of the O_2 molecule is carefully investigated with a variety of VB methods and with different quality basis sets. The best binding energy, obtained with the VBCISD method and the cc-pVTZ basis set, amounts to 110.0 kcal/mol at the internuclear distance of 2.336 bohr, whereas a VBSCF computation with 105 structures yields a binding of 77.71 kcal/mol, to be compared with the experimental value of 120.6 kcal/mol at 2.2819 bohr (see Table 1). Total energies are not reported.⁹⁴ From Table 3, I see that only one HF function and one HL covalent structure, the simple HF–HL computation, yields a binding energy of 62.26 and 65.88 kcal/mol with the (HF–HL)(1,1) and the (HF*–HL)(1,1), respectively. The (HF–HL)(1,3) with 4 HL structures (see Table 2) yields 76.56 kcal/mol, whereas the value is 82.40 kcal/mol with the (HF*–HL)(1,3). Finally, I obtain 110.12 and 115.02 kcal/mol with the HF–HL- i and the HF*–HL- i , respectively. This comparison indicates that the new HF–HL method is competitive with modern VB computations.^{35,94}

The addition of ionic structures in F_2 brings to a computed binding energy of 35.70 kcal/mol for HF–HL- i and to 38.71 kcal/mol for HF*–HL- i , close to the experimental value; note that this value takes into account the stabilization energy at dissociation, 2.35 kcal/mol, due to the split of the 2p electrons

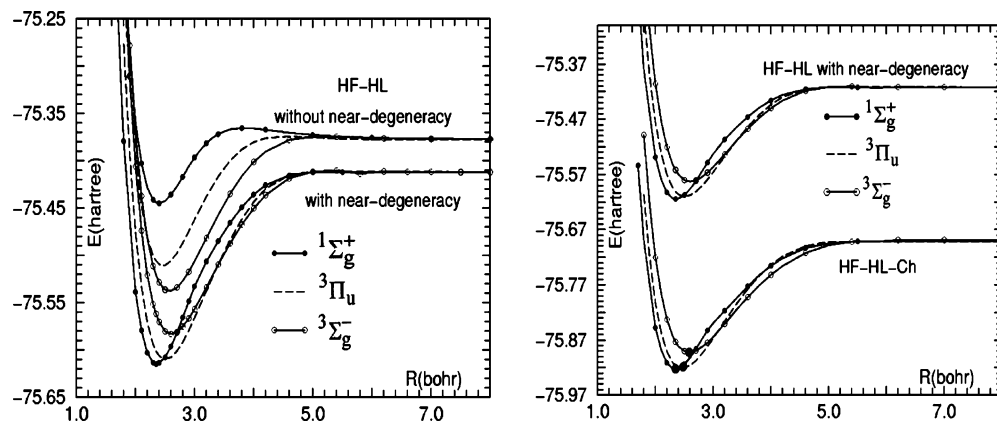


Figure 3. Potential energy for the three lowest states of C_2 . Left: Computations from HF–HL without and with near degeneracy. Right: Computations from HF–HL with near degeneracy and HF–HL-Ch; bullets for the exact nonrelativistic energy at equilibrium and dissociation.

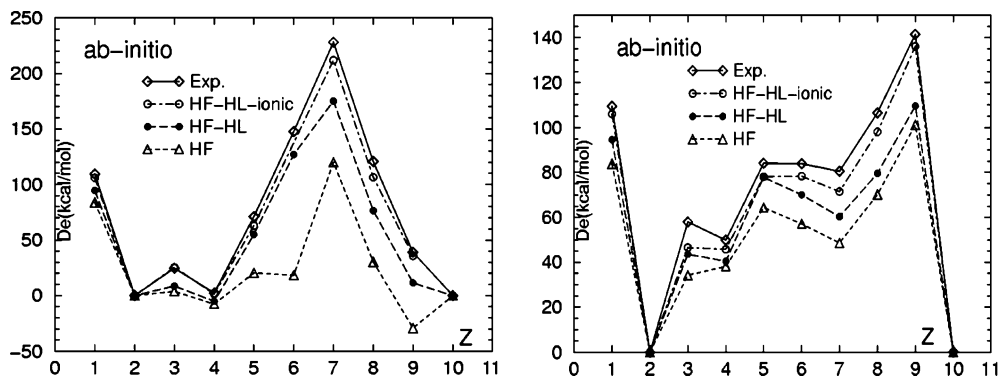


Figure 4. Binding energy (kcal/mol): values from experiments and from HF–HL-i, HF–HL, and HF computations. Left for homopolar molecules. Right for hydride molecules.

of the atomic spherical symmetry at dissociation into the $2p_\sigma$ and $2p_\pi$ in the linear field of the molecule (as discussed in ref 45 and at the end of the next section).

In the left inset of Figure 4, I report the computed binding energies at equilibrium from HF, (HF–HL)(S,T), (HF–HL-i)(S,T), and the laboratory values. In the right inset, I report the corresponding quantities for the diatomic hydride molecules, to provide a more general comparison of ab initio HF–HL computations. The quality of the three computational levels, HF, HF–HL, and HF–HL-i, and the relative improvements are clear from the figure. Note, in addition, that in the inset for the homopolar I have not included the improvement obtained with $E_b(\text{HF}^*-\text{HL})$ and $E_b(\text{HF}^*-\text{HL-i})$, because these are not computed for the hydrides. I conclude that the computations are rather unreliable, even qualitatively at the HF level, but become qualitatively reliable at the HF–HL level, and quantitatively realistic at the HF–HL-i level. The error in the computed binding energy, the extra correlation energy, η_{model} of eq 7, is illustrated in Figure 5 for different models. From the figure, it is evident that in binding energy calculations, the correlation energy varies notably from model to model. As expected, the residual error (related to $\omega_{ij}(\text{dyn})$ discussed for eq 6) is proportional to the number of binding electron pairs; thus it is a maximum for N_2 .

As previously stated, the small remaining error in $E_b(\text{HF}-\text{HL-i})$ can be accounted for by adding a few well-chosen structures to the HF–HL-i function to introduce inter-pair correlation energy ($\omega_{ij}(\text{dyn})$ of eq 6). However, rather than follow this ab initio approach, which requires adding more terms in the HF–HL expansion, I use a semiempirical density functional to scale the energy to accurate nonrelativistic values.

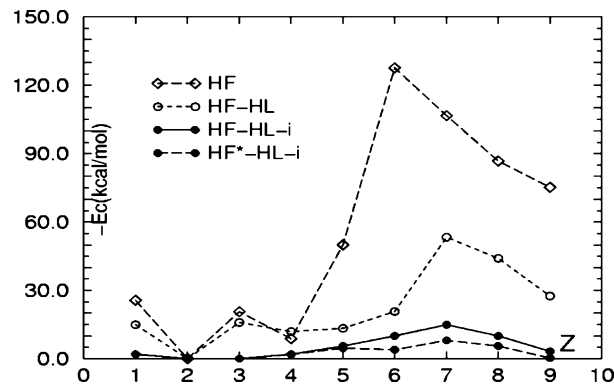


Figure 5. Residual binding energy error (i.e., the molecular extra correlation, η_{model}) for the HF, HF–HL, HF–HL-i, and HF*–HL-i models.

5. Computation of the Atomic Dynamical Correlation Energy

Once the HF–HL wave function is computed, the largest energy correction that remains to be included is $\sum_a \epsilon_a(\text{dyn})$ (see eq 5). As $\epsilon_a(\text{dyn})$ is a simple and regular function of the atomic number Z , the functional task is not as complex as in DFT computations, so it can be represented by the soft Coulomb hole, Ch, density functional approximation.^{44,45,53–58} In the soft Coulomb hole approximation, the operator $1/r_{ij}$ is replaced with $(1 - e^{-\alpha r_{ij}^2})/r_{ij}$, where α is a semiempirical parameter. As shown in previous papers, the choice of the Coulomb hole algorithm is not unique. Therefore, different functionals, such as those in ref 83, could have been used after being recalibrated for the HF–HL model.

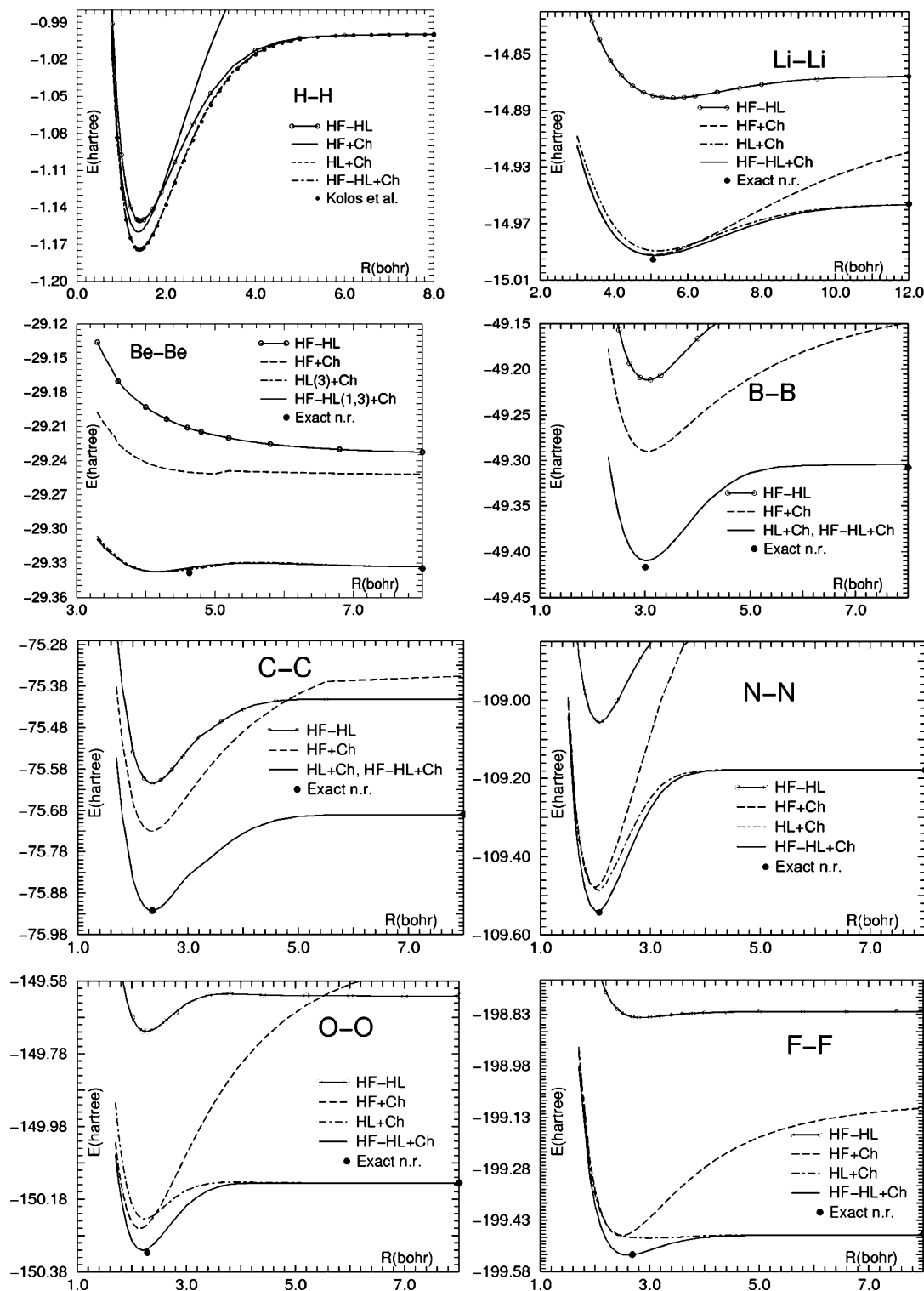


Figure 6. Coulomb hole computations. HF-Ch, HL-Ch, and (HF–HL)-Ch potential energy curves for the ground state of H_2 , Li_2 , Be_2 , B_2 , C_2 , N_2 , O_2 , and F_2 .

Computed total energies from the HF–HL function corrected with the Ch functional are collected in Table 4, and the corresponding potential energy curves are given in Figure 6. In the figure, I have included the HF-Ch and the HL-Ch potential energy curves obtained from the HF and HL wave functions, and a portion of the HF–HL potential curve near equilibrium is displayed for comparison. There are small deviations from experiments for F_2 and Be_2 , but the overall resulting trend is satisfactory, particularly as it is obtained with the ab initio HF–HL wave function, which yields nearly correct binding energy,

and with a scaling of the total energy using the soft Coulomb hole algorithm. This confirms the trend I previously reported for single bond molecules.

Note that it is easier to account for $\sum_a \epsilon_a(\text{dyn})$ than for $E_c(\text{dyn})$, because $\eta(\text{dyn})$ depends on the chosen computational model (for the HF–HL model, it is smaller than the HF and the HL models, but still substantial) and varies from molecule to molecule at each internuclear distance. On the other hand, for a given electronic configuration, $\epsilon_a(\text{dyn})$ is a relatively simple and well-behaved function⁵⁸ of the atomic number Z , which is

TABLE 4: Coulomb Hole Functional Energies: Binding (kcal/mol), $E_b(\text{HF-HL})\text{Ch}$, Total (hartree), $E_t(\text{HF-HL})\text{Ch-R}_e$, $E_t(\text{HF-HL})\text{Ch-R}_\infty$, Errors ΔE_b (kcal/mol) and $\Delta E_{t\infty}$ (mhartree), and Computed Equilibrium Distance (bohr), R_e

molecule	$E_b(\text{HF-HL})\text{Ch}$	$-E_t(\text{HF-HL})\text{Ch-R}_e$	$-E_t(\text{HF-HL})\text{Ch-R}_\infty$	ΔE_b	$\Delta E_{t\infty}$	R_e
H ₂ [$^1\Sigma_g^+$]	109.48	1.17448	1.00000	0.00	0.00	1.40
He ₂ [$^1\Sigma_g^+$]	0.02	5.807470	5.807436	0.00	0.00	6.25
Li ₂ [$^1\Sigma_g^+$]	22.95	14.99253	14.95596	-1.74	-0.02	5.111
Be ₂ [$^1\Sigma_g^+$]	2.09	29.33761	29.33427	-0.31	-0.05	4.167
B ₂ [$^3\Sigma_g^-$]	66.41	49.41007	49.30423	-2.11	-3.57	3.025
C ₂ [$^1\Sigma_g^+$]	147.44	75.92379	75.68883	-0.41	-1.17	2.348
N ₂ [$^1\Sigma_g^+$]	227.83	109.54025	109.17717	-1.11	-1.43	2.041
O ₂ [$^3\Sigma_g^-$]	116.91	150.32046	150.13415	-3.72	-0.65	2.191
F ₂ [$^1\Sigma_g^+$]	39.86	199.53180	199.46827	0.86	-0.07	2.603
Ne ₂ [$^1\Sigma_g^+$]	0.08	257.875856	257.875723	0.00	-0.88	6.40

nearly constant at different internuclear separations. Furthermore, the semiempirical parametrization ensures a best fit to the “exact nonrelativistic energies”, as detailed in previous work.^{44,45}

In Table 4, I report the computed binding energy at equilibrium, $E_b(\text{HF-HL})\text{-Ch}$, the total energy at equilibrium, $E_t(\text{HF-HL})\text{-Ch-R}_e$, and dissociation, $E_t(\text{HF-HL})\text{-Ch-R}_\infty$, the error in the computed binding energy, ΔE_b , and in the total energy at dissociation, $\Delta E_{t\infty}$, relative to accurate nonrelativistic values (see Table 1), and the equilibrium distance, R_e . The data from the computed binding energy either from $E_b(\text{HF-HL-i})$ or from $E_b(\text{HF-HL})\text{-Ch}$ show that the computational technique I have proposed yields reasonable or accurate values. This is highlighted in Figure 7 where I compare the experimental and the (HF-HL)-Ch binding energies both for the homopolar molecules and for the diatomic hydrides.

For the C₂ excited states, (HF-HL)-Ch computations yield, at equilibrium, total energies of -75.92009 and -75.89203 hartree, for the $^3\Pi_u$ and the $^3\Sigma_g^-$ states, respectively. The ground-state total energy is -75.92379 hartree (see Table 4 and right inset of Figure 3), leading to the excitation energies of 0.10 and 0.82 eV, for the $^3\Pi_u$ and $^3\Sigma_g^-$; the corresponding experimental values^{84,88} are 0.10 and 0.96 eV. The good agreement between computed and experimental electronic excitation is in line with previous results⁴³ for an excited state in LiH.

To complete the tabulation for the homopolar molecules, I add very preliminary computations for He₂ and Ne₂; the HF-HL(1,1) total energies at the experimental equilibrium separation and at dissociation are -5.723331 and -5.723359 hartree for He₂ and -257.094010 and -257.094104 hartree for Ne₂. The computations with HF-HL-Ch (see Table 4) show a minimum, but at larger internuclear separation than experimentally observed.

Concerning the computed binding energies at dissociation, I recall that, due to the molecular symmetry, the 2p electrons are split into 2p_σ different from 2p_π; for the separated atom (in spherical symmetry), there is no such splitting. This causes some correlation energy gain (due to the use of different orbitals for different spins) in the molecule but not in the separated atoms.⁹⁵ This energy gain is not negligible and amounts to ~2.5 kcal/mol in F₂. The molecular energy at a very large distance (considered “dissociation distance”) is required to match the sum of the separated atoms by constraining the basis set coefficients of the 2p_σ orbitals to be degenerate to the 2p_π orbitals;⁴⁵ the imposed constraint notably improves the energy matching of the linear and spherical symmetry computations (compare the data at dissociation of Table 4 with the equivalent data in Table 1).

6. Conclusions

The goal of this work is to compare my model with laboratory data. However, I have included a brief summary of some recently published computational results to provide a comparison of the results of my approach with those models.

Quantum Monte Carlo, QMC, computations are known to providing reliable energies. However, computations⁹⁶ with diffusion QMC for the ground state of Li₂, Be₂, B₂, C₂, N₂, O₂, and F₂ performed at the experimental internuclear separation underestimate the energy by 0.00162, 0.00848, 0.01899, 0.03543, 0.0375, 0.0499, and 0.0434 hartree, respectively, as compared to the exact nonrelativistic energies given in Table 1. Thus, they are marginally more accurate than my value for Li₂ (see Table 4) but somewhat worse for the remaining molecules. This is also true for more recent work⁹⁷ where the deviations are 0.00062, 0.025, and 0.0223 hartree for Li₂, C₂, and N₂,

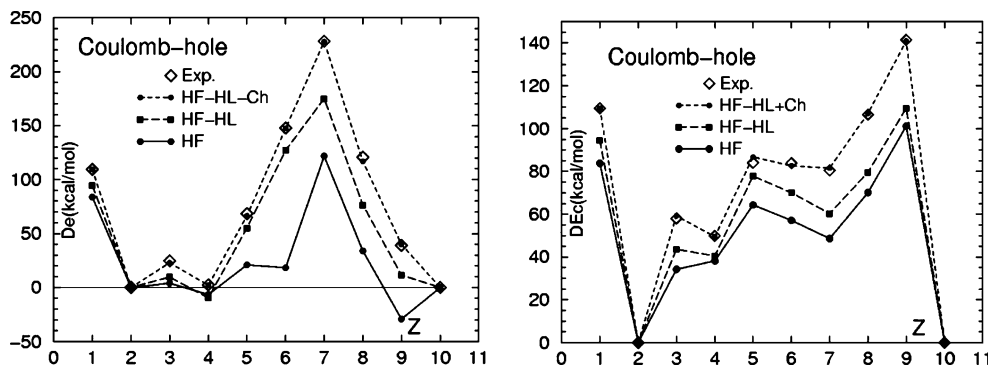


Figure 7. Experimental and (HF-HL)-Ch, HF-HL, and HF binding energies for homopolar diatomic molecules (left inset) and for diatomic hydrides (right inset).

respectively. Hylleraas CI computations,^{98,99} with explicit $1/r_{12}$ correlation factors, performed for Be₂ and N₂, report total energies underestimated by 0.00594 hartree for N₂ and by 0.06697 hartree for Be₂ (note in ref 98 the very accurate computed binding energy for Be₂, 2.58 kcal/mol, and a discussion on the errors of experimental binding energies). Recent full CI computations^{100,101} for N₂ report a total energy of -109.3753 hartree with a very extended number of SD-NO¹⁰⁰ and a total energy,¹⁰¹ with frozen core, of -109.278339 hartree, the latter with a binding energy of 201.55 kcal/mol. Another extended set of computations¹⁰² yields the total energies of -75.81445 , -109.42505 , -150.20396 , and -199.39929 for C₂, N₂, O₂, and F₂, to be compared to the data in Table 4. A coupled cluster computation¹⁰³ for F₂ reports a total energy of -199.102796 , and another FCI computation for N₂ reports¹⁰⁴ a total energy of -109.3754 hartree. A recent publication¹⁰⁵ on C₂ establishes the computational accuracy limit, particularly for coupled cluster techniques, and contains extensive tabulation for binding energy and other properties.

From this limited summary, one can appreciate the accuracy achieved by today's computational chemistry and also realize that the infant HF–HL model is a reasonable alternative. Admittedly, the use of the semiempirical Coulomb hole algorithm favors the HF–HL computations in the above comparison.

The computational performance of the HF–HL method can be assessed by comparison to the well-known HF and MC–HF^{1,2,106} and VB methods.^{35,65} The bottleneck for the HF–HL, VB, and nonorthogonal CI¹⁰⁷ is the lack of more efficient algorithms for the orbital optimization.

In general, the HF–HL method is computationally competitive with most VB methods, because it requires shorter expansions and uses essentially equivalent algorithms. However, it falls behind MC–HF approaches, despite the shorter expansions, because of the orthogonality of the MC–HF orbitals. The importance of short expansions has been stressed in the natural orbital and in the VB literature, particularly as a way to provide a chemical interpretation on quantum chemical computations.

Recently, I have included⁶⁷ efficient optimization techniques and shortened the orbital coefficient list by switching from Gaussian to Slater-type functions;¹⁰⁸ tests of these improvements are in progress on computations of the CO ground state.⁶⁷ However, I hope that transfer of HF–HL bond representations from small to larger molecules will eventually become a way to deal with HF–HL in large molecular systems. Further algorithmic improvements in nonorthogonal CI and VB methods will also improve the HF–HL performance.

In conclusion, I have discussed the application of a new computational method, the Hartree–Fock–Heitler–London, and compared Hartree–Fock, Heitler–London, and Hartree–Fock–Heitler–London potential energy curves for the first and second period homonuclear molecules. The present results confirm the conclusion obtained from the study on the diatomic hydrides:^{42–45} the HF–HL method leads to realistic binding energies with relatively few configurations and to accurate total energies with density functionals.

Neither the HF nor the HL approximations are capable of systematically reproducing, at least qualitatively, the basic molecular binding features known experimentally (bond breaking and bond formation). However, the two traditional methods have provided the foundation for many concepts in physical chemistry and in chemical physics. Their sound basic qualities of mathematical simplicity and immediate physical interpret-

ability have historically provided two distinct quantum chemical models for theoretical and computational chemistry.

The HF–HL method merges the two historical paths, with a marginal increase in computational complexity, while retaining the easy physical interpretability of the two traditional proposals.

I stress that the computations validate the notion^{44,45} that the two traditional methods, HF and HL, are both required to satisfactorily describe the evolution of the electronic structure in a chemical bond from molecular dissociation to the united atom.

The limited number of configurations and structures given in Table 2, which yield the realistic binding energies reported in Figures 4 and 7, stand in stark contrast to the typical expansion length of CI computations and remind us of the proposals originated by Löwdin²¹ and continued by his school, where canonical atomic and molecular orbitals are replaced by new formulations, including natural,^{23,24} alternant,²⁵ Dayson^{26,27} orbitals, nonorthogonal CI,¹⁰⁷ and geminals.²⁸

Acknowledgment. This work was partially presented with note distribution in October 2006 at the Chemistry Departments of the Peking, Sichuan, Xiamen, Shanghai Jiao Tong, Hong Kong Universities and of the Chinese Academy of Sciences in Beijing, and in April 2007 to the Chemistry Departments at the Universities of Stockholm, Uppsala, Lund, and Aarhus. It is a pleasure to thank Prof. Dr. Enrico Clementi for suggestions, discussions, and for providing some of the computational facilities, and Dr. Fiona Sim for proofreading the manuscript. Finally, a grant from MIUR-2004034838 is acknowledged.

References and Notes

- (1) *Fundamental Work of Quantum Chemistry*; Brändas, E. J., Kryachko, E. S., Eds.; Kluwer Academic: Boston, 2003.
- (2) *Theory and Applications of Computational Chemistry: The First 40 Years*; Dykstra, C. E., Frenking, G., Kim, K. S., Scuseria, G. E., Eds.; Elsevier: Amsterdam, 2005.
- (3) Hund, F. R. *Z. Phys.* **1927**, *40*, 742.
- (4) Mulliken, R. S. *Phys. Rev.* **1928**, *32*, 186.
- (5) Herzberg, G. *Spectra of Diatomic Molecules*; D. Van Nostrand: Princeton, NJ, 1951 and references thereby given.
- (6) Heitler, W.; London, F. *Z. Phys.* **1927**, *44*, 455.
- (7) Hartree, D. R. *Proc. R. Soc. A* **1933**, *141*, 269 and references thereby given.
- (8) Fock, V. *Z. Phys.* **1930**, *62*, 795.
- (9) Roothaan, C. C. *J. Rev. Mod. Phys.* **1951**, *23*, 69.
- (10) Roothaan, C. C. *J. Rev. Mod. Phys.* **1960**, *32*, 179.
- (11) Sherrill, D. C.; Schaefer, H. F., III. *Adv. Quantum Chem.* **1999**, *34*, 143.
- (12) Shavitt, I. *Adv. Quantum Chem.* **1999**, *34*, 189.
- (13) Hartree, D. R.; Hartree, W.; Swirles, B. *Trans. R. Soc.* **1939**, *299*, 238.
- (14) Shepard, R. *Adv. Chem. Phys.* **1987**, *69*, 6.
- (15) Sabelli, N.; Hinze, J. *J. Chem. Phys.* **1969**, *50*, 684.
- (16) Roos, B. O.; Siegbahn, P. E. In *Modern Theoretical Chemistry*; Schaefer, H. F., III, Ed.; Plenum Press: New York, 1977.
- (17) Roos, B. O. In *Methods in Computational Molecular Physics*; Diercksen, G. H. F., Wilson, S., Eds.; Reidel: Dordrecht, 1984.
- (18) Andersson, K.; Barysz, M.; Bernhardsson, A.; Blomberg, M. R. A.; Cooper, D. L.; Fulscher, M. P.; da Graaf, C.; Hess, B. A.; Karlstrom, G.; Lindh, R.; Malmqvist, P.-A.; Nakjima, T.; Neogard, P.; Olsen, J.; Roos, B. O.; Schimmelpfennig, B.; Shutz, M.; Seijo, L.; Serrano-Andres, L.; Siegbahn, P. E. M.; Stalrig, J.; Thorsteinsson, T.; Veryazov, V.; Widmark, P.-O. *MOLCAS*, Version 5.4; Lund, Sweden, 2002.
- (19) Helgaker, T.; Jensen, H. Ja. Aa.; Jørgensen, P.; Olsen, J.; Ruud, K.; Ågren, H.; Anderson, T.; Bak, K. L.; Bakken, V.; Christiansen, O.; Dahle, P.; Dalskov, E. K.; Enevoldsen, T.; Fernandez, B.; Heiberg, H.; Hettema, H.; Jonsson, D.; Kirpekar, S.; Kobayashi, R.; Koch, H.; Mikkelsen, K. V.; Norman, P.; Packer, M. J.; Saue, T.; Taylor, P. R.; Vahtras, O. *DALTON, an ab initio electronic structure program, Release 1.0*; Norway, 1997.
- (20) Peyerimhoff, S. D.; Buenker, R. J. In *Excited States in Chemistry*; Nikolaidis, C. A., Beck, D. R., Eds.; Reidel: Dordrecht, 1978; p 79.
- (21) Löwdin, P.-O. *Adv. Chem. Phys.* **1959**, *2*, 207.
- (22) Davidson, E. R. *Rev. Mod. Phys.* **1972**, *44*, 451.

- (23) Thulstrup, E. W.; Öhrn, Y. *J. Chem. Phys.* **1972**, *57*, 3716.
- (24) Bagus, P. S.; Moser, C. M.; Goethals, P.; Verhagen, G. *J. Chem. Phys.* **1973**, *58*, 1886.
- (25) Pauncz, R. *Alternant Molecular Orbitals Method*; Saunders: Philadelphia, PA, 1967.
- (26) Linderberg, J.; Öhrn, Y. *Propagators in Quantum Chemistry*; Academic Press: New York, 1973.
- (27) Ortiz, J. V. *Advances in Quantum Chemistry 35*; Academic Press: New York, 1999.
- (28) Polly, R.; Werner, H.-J.; Taylor, P. R. *J. Chem. Phys.* **2006**, *124*, 234107.
- (29) Pauling, L. *J. Am. Chem. Soc.* **1931**, *53*, 1357.
- (30) Slater, J. C. *Phys. Rev.* **1932**, *33*, 255.
- (31) Wheland, G. W. *Resonance in Organic Chemistry*; Wiley: New York, 1955 and references thereby given.
- (32) Bobrowic, F. B.; Goddard, W. A. In *Methods of Electronic Structure Theory*; Schaefer, H. F., III, Ed.; Plenum: New York, 1977; p 79.
- (33) Cooper, D. L.; Gerratt, J.; Raimondi, M. In *Valence Bond Theory and Chemical Structure*; Klein, D. J., Trinajstić, N., Eds.; Elsevier: New York, 1990; p 287.
- (34) Hiberty, P. C.; Humbel, S.; Byrman, C. P.; van Lenthe, J. H. J. *J. Chem. Phys.* **1994**, *101*, 407.
- (35) Special Issue, 90 Years of Chemical Bonding. *J. Comput. Chem.* **2007**, *28*.
- (36) Hiberty, P. C.; Shaik, S. *J. Comput. Chem.* **2007**, *28*, 137.
- (37) Hammond, B. L.; Lester, W. A., Jr.; Reynolds, P. J. *Monte Carlo Methods in Quantum Chemistry*; World Scientific: Singapore, 1994.
- (38) Hohenberg, P.; Kohn, W. *Phys. Rev. B* **1964**, *136*, 864.
- (39) See, for example: Parr, R. G.; Yang, W. *Density functional theory of atoms and molecules*; Oxford University Press: Oxford, 1985.
- (40) Nakano, H.; Nakajima, T.; Tsuneda, T.; Hirao, K. In *Theory and Applications of Computational Chemistry: The First 40 Years*; Dykstra, C. E., Frenking, G., Kim, K. S., Scuseria, G. E., Eds.; Elsevier: Amsterdam, 2005; Chapter 20.
- (41) Clementi, E. In *Fundamental Work of Quantum Chemistry*; Brändas, E. J., Kryachko, E. S., Eds.; Kluwer Academic: Boston, 2003; Chapter 6.
- (42) Corongiu, G. *Int. J. Quantum Chem.* **2005**, *105*, 831.
- (43) Corongiu, G. *J. Phys. Chem. A* **2006**, *110*, 11584.
- (44) Clementi, E.; Corongiu, G. *Theor. Chem. Acc.* **2007**, *118*, 453.
- (45) Corongiu, G. *J. Phys. Chem. A* **2007**, *111*, 5333.
- (46) Sinanoglu, O. *J. Chem. Phys.* **1962**, *36*, 706.
- (47) Sinanoglu, O. *Adv. Chem. Phys.* **1964**, *6*, 315.
- (48) Mc Koy, V.; Sinanoglu, O. *J. Chem. Phys.* **1964**, *41*, 2689.
- (49) Clementi, E.; Veillard, A. *J. Chem. Phys.* **1966**, *44*, 3050.
- (50) Bagus, P. S.; Moser, C. M. *Phys. Rev.* **1968**, *167*, 13.
- (51) Veillard, A.; Clementi, E. *J. Chem. Phys.* **1968**, *49*, 2415.
- (52) Majorana, E. *Rend. Acc. Lincei* **1931**, *13*, 58.
- (53) Clementi, E. *IBM J. Res. Dev.* **1965**, *9*, 2.
- (54) Chakravorty, S.; Clementi, E. *Phys. Rev. A* **1989**, *39*, 2290.
- (55) Clementi, E.; Corongiu, G. *Int. J. Quantum Chem.* **1997**, *62*, 572.
- (56) Clementi, E.; Hofmann, D. W. *Int. J. Quantum Chem.* **1994**, *52*, 849.
- (57) Clementi, E.; Corongiu, G. *Chem. Phys. Lett.* **1998**, *282*, 335.
- (58) Corongiu, G., in preparation.
- (59) Chakravorty, S. J.; Davidson, E. R. *J. Phys. Chem.* **1996**, *100*, 6167.
- (60) Pauncz, R. *The Symmetric Group in Quantum Chemistry*; CRC Press, Inc.: Boca Raton, FL, 1995.
- (61) Wigner, E.; Witmer, E. E. *Z. Phys.* **1928**, *51*, 859.
- (62) Löwdin, P.-O. *Phys. Rev.* **1955**, *97*, 1474.
- (63) Slater, J. C. *Theory of Molecules and Solids, Vol. 1, Electronic Structure of Molecules*; McGraw-Hill: New York, 1963.
- (64) Prosser, F.; Hagstrom, S. *J. Chem. Phys.* **1968**, *48*, 4807.
- (65) *Valence Bond Theory*; Cooper, D. L., Ed.; Elsevier: Amsterdam, 2002.
- (66) Leasure, S. C.; Balint-Kurti, G. G. *Phys. Rev. A* **1985**, *31*, 2107.
- (67) Corongiu, G.; Fernandez Rico, J., to be published.
- (68) Wigner, E. *Phys. Rev.* **1934**, *46*, 1002.
- (69) Nesbet, R. K. *Adv. Chem. Phys.* **1965**, *9*, 321.
- (70) Clementi, E. *J. Chem. Phys.* **1962**, *36*, 33.
- (71) Linderberg, J.; Shull, H. J. *Mol. Spectrosc.* **1960**, *5*, 1.
- (72) Ehara, M.; Hasegawa, J.; Nakatsuji, H. In *Theory and Applications of Computational Chemistry: The First 40 Years*; Dykstra, C. E., Frenking, G., Kim, K. S., Scuseria, G. E., Eds.; Elsevier: Amsterdam, 2005; Chapter 39.
- (73) Herzberg, G. *Spectra of Diatomic Molecules*; D. Van Nostrand: Princeton, NJ, 1951; Chapter VI.
- (74) Mulliken, R. S. In *The Interpretation of Band Spectra, Part III*; Mulliken, R. S., Ramsey, D. A., Hinze, J., Eds.; The University of Chicago Press: Chicago, IL, 1975.
- (75) Valderrama, E.; Ludeña, E. V.; Hinze, J. *J. Chem. Phys.* **1999**, *110*, 2343.
- (76) Mok, D. K. W.; Neuman, R.; Handy, N. C. *J. Phys. Chem.* **1996**, *100*, 6225.
- (77) Bagus, P. S.; Broer, R.; Parmigiani, F. *Chem. Phys. Lett.* **2006**, *421*, 148.
- (78) Gombas, P. *Die Statistische Theorie des Atoms und ihre Anwendungen*; Springer-Verlag: Wien, 1949.
- (79) Gombas, P. *Pseudopotential*; Springer-Verlag: New York, 1967.
- (80) Gombas, P. *Acta Phys.* **1961**, *13*, 233.
- (81) Gombas, P. *Acta Phys.* **1962**, *14*, 83.
- (82) Clementi, E. *Proc. Natl. Acad. Sci. U.S.A.* **1972**, *69*, 2942.
- (83) Clementi, E.; Corongiu, G.; Stradella, O. G. In *MOTECC 1991*; Clementi, E., Ed.; ESCOM: Leiden, 1991; Chapter 8.
- (84) Huber, K. P.; Herzberg, G. *Molecular Spectra and Molecular Structure IV. Constants of Diatomic Molecules*; Van Nostrand Reinhold: New York, 1979.
- (85) Kolos, W. K.; Szalewicz, K.; Monkhorst, H. J. *J. Chem. Phys.* **1986**, *84*, 3278.
- (86) Anderson, J. B. *J. Chem. Phys.* **2004**, *120*, 9886.
- (87) Kaledin, L. A.; Kaledin, A. L.; Heaven, M. C.; Bondybey, V. E. *THEOCHEM* **1999**, *177*, 461.
- (88) Chase, M. W., Jr.; Davis, C. A.; Douney, C. A., Jr.; Frurip, D. J. R.; Donald, R.; Syverud, A. N. *J. Phys. Chem. Data* **1985**, *14*, Suppl. 1.
- (89) Urdhal, R. S.; Bao, Y.; Jacson, W. M. *Chem. Phys. Lett.* **1991**, *178*, 425.
- (90) Aziz, R. A.; Slaman, M. *J. Chem. Phys.* **1989**, *130*, 187.
- (91) Das, G.; Wahl, A. C. *J. Chem. Phys.* **1966**, *44*, 87.
- (92) Lie, G. C.; Clementi, E. *J. Chem. Phys.* **1974**, *60*, 1288.
- (93) Roos, B. O. In *Ab initio Methods in Quantum Chemistry, Part II*; Lawley, K. P., Ed.; John Wiley and Sons: New York, 1987; p 399.
- (94) Su, P.; Song, L.; Wu, W.; Hiberty, P. C.; Shaik, S. *J. Comput. Chem.* **2007**, *28*, 185.
- (95) Bagus, P. S., private communication.
- (96) Filippi, C.; Umrigar, C. J. *J. Chem. Phys.* **1996**, *105*, 213.
- (97) Lüchow, A.; Fink, R. F. *J. Chem. Phys.* **2000**, *113*, 8457.
- (98) Gdanitz, R. *J. Chem. Phys. Lett.* **1998**, *283*, 253.
- (99) Gdanitz, R. *J. Chem. Phys. Lett.* **1999**, *312*, 578.
- (100) Bytautas, L.; Ruedenberg, K. *J. Chem. Phys.* **2004**, *121*, 10919.
- (101) Larsen, H.; Olsen, J.; Jorgensen, P. *J. Chem. Phys.* **2000**, *113*, 6677.
- (102) Bytautas, L.; Ruedenberg, K. *J. Chem. Phys.* **2005**, *122*, 154110.
- (103) Kowalski, K.; Piecuch, P. *Chem. Phys. Lett.* **2001**, *344*, 165.
- (104) Köhn, A.; Olsen, J. *J. Chem. Phys.* **2006**, *125*, 174110.
- (105) Feller, D.; Peterson, K. A. *J. Chem. Phys.* **2007**, *126*, 114105.
- (106) *Modern Method and Algorithms of Quantum Chemistry*; Grotdorfer, J., Ed.; von Neumann Inst.: Jülich, 2000; Vol. 3.
- (107) Broer, R.; Van Oosten, A. B.; Nieuwpoort, W. C. *Rev. Solid State Sci.* **1992**, *5*, 79.
- (108) Fernandez Rico, J.; Lopez, R.; Ema, I.; Ramirez, G. *J. Comput. Chem.* **2004**, *25*, 1987.